

Respiratory tract evaluation in COVID-19 patients using multifrequency electrical impedance tomography and 2D D-Bar reconstruction

Julia Grasiela Busarello Wolff
Programa de Pós-Graduação em
Engenharia Elétrica
Universidade do Estado de Santa
Catarina
Joinville, Brazil
ORCID: 0000-0002-3536-5611

Pedro Bertemes-Filho
Programa de Pós-Graduação em
Engenharia Elétrica
Universidade do Estado de Santa
Catarina
Joinville, Brazil
ORCID: 0000-0002-5264-4874

Wellington Pinheiro dos Santos
Programa de Pós-Graduação em
Engenharia Biomédica
Universidade Federal de Pernambuco
Uberlândia, Brazil
ORCID: 0000-0003-2558-6602

Abstract— Originated in December 2019 in the city of Wuhan, COVID-19 has become the biggest public health problem in the past hundred years. Although its mortality is not proportionally as high when compared to other infectious diseases, COVID-19 is a highly infectious disease, having already infected more than 200 million people worldwide, with more than three million deaths. Intensive care units and resources from public health systems are being exhausted. In its severe form, COVID-19 can cause thrombosis, cytopenias and other problems caused by early clotting, in addition to great damage to the respiratory tract. Monitoring of pulmonary function in moderate and severe patients is of fundamental importance for assessing the severity of the disease and the evolution of treatment. Multifrequency electrical impedance tomography can be used as a low-cost method for monitoring pulmonary function by imaging. In this work we propose a system for monitoring the image of the lungs in patients positive for COVID-19 or with severe acute respiratory syndrome using electrical impedance tomography and the 2d D-Bar image reconstruction method. The results are presented as a proof of concept using numerical phantoms that represent the lungs, the heart and other adjacent structures using radial sections. The experimental results show that a low-cost electrical impedance tomography system with 16 electrodes can be used to generate functional images of the respiratory system useful for monitoring respiratory function in a non-invasive way.

Keywords — D-Bar Method, Electrical Impedance Tomography, COVID-19, Imaging, Simulations.

I. INTRODUCTION

Multifrequency electrical impedance tomography (MfEIT) uses electrical characteristics intrinsic to human organs to describe respiratory [1], cardiological [2], cerebral [3], hemodynamic behavior [4], emptying of the stomach [5], pulmonary process in cases of COVID-19 pneumonia [6], applications in plethysmography [7] and also the evolution of cancerous pathologies [8] by images. It can also be used for planning therapies in which external electrical currents are injected into the human body, such as defibrillation [9] and cardiac stimulation [10], among many other applications. This tool uses current and limit voltage to provide information about the spatial distribution of impedance, resistivity, permittiveness or electrical conductivity. One of the biggest problems of Electrical Impedance Tomography (EIT) was the inaccessibility of the internal voltage or current data to find

the real values of the internal impedance in the visualized tissues.

During the 40 years of study of this technique, many numerical methods have been proposed to solve the direct problem and the inverse problem. In direct problems, we discretize the region under analysis into small sub-regions, usually using the finite element method.

In the case of inverse problems, either there is no single solution or the solution is not continuously dependent on the data. This leads us to methods of regularization and optimization, such as singular value decomposition - SVD, average least squares - LMS, Tikhonov regularization method, Monte Carlo optimization method, etc.

The solution of the impedance distribution in MfEIT is an inverse, non-linear, underdetermined, poorly placed and poorly conditioned problem, which requires the use of a regularization method. The generalized methods of Tikhonov regularization have been popular in solving many inverse problems. The regularization matrices generally used with the Tikhonov regularization method are intended for this purpose, and the a priori premises are implicit, therefore, in many cases, they are inadequate, as they generate images that do not correspond to the real image, of the object under analysis.

The insensitivity inherent to the circumference measurements of the deep tissue impedance and the non-linearity of the current flows have been the main problems for obtaining useful images.

The algorithms to solve the inverse problem in EIT presented in the literature are:

- Tikhonov realization method [11], [12], [13].
- Sparse regularization method [14], [15], [16].
- Multiplicative regularization method [17].
- Regularized reconstructor of spectral modeling [18].
- Gauss-Newton method [19], [20].
- Modified Newton-Raphson method and Geselowitz sensitivity theorem [21].
- D-Bar Method [22], [23], [24], [25], [26].

The computational complexity of the EIT has severe practical limitations. The reverse problem is typically poorly conditioned and requires simplified assumptions or the algorithm must be based on regularization with prior knowledge. Due to the poor conditioning of the inverse problem, the limits of the internal organs of the Organs are usually blurred or out of focus in the reconstructed image. For

this reason, the image reconstruction algorithms continue to be improved and new methods suggested and tested, in order to avoid this discomfort in the images, as they can lead to errors in medical diagnosis.

However, among the researched methods, the one that showed the best performance preserving the contour of the domain and generating higher quality images was the D-Bar method.

The D-Bar method for EIT was developed in the years 1999 and 2000, in Finland and in the United States, and has been improved since then [26], [27]. It is based on Fourier nonlinear transforms, customized for each case, involving current and voltage measurement data. Low-pass filtering in the nonlinear Fourier domain is used to stabilize the reconstruction process. The D-Bar method for two-dimensional images has shown to be very promising in providing robust reconstructions of absolute conductivity and time difference, in real time, but have not yet been used in practical electrode data for three-dimensional images until 2020 [25], [27].

Dood and Mueller (2014) evaluated the feasibility of using a rapid implementation of the two-dimensional D-Bar method for EIT, with reconstructions of the conductivity changes in the chest, in real time. The images of the transverse differences of a healthy human chest are presented and are the first D-Bar images of human data collected from an EIT system, with current injection applied to pairs of electrodes [28].

According to Adler and Boyle (2017) the reconstruction approach by iterative methods, with some regularization, is the most common technique in the literature [20]. However, the D-Bar method showed more interesting results and, for this reason, it was listed to be used in this work. The poor conditioning is due to the discretization of Fredholm's Integral Equation, which makes the problem poorly placed, since the existence and uniqueness of the solution to the problem are not always guaranteed.

In 2020, the world was surprised by the rapid spread of the SARS-CoV-2 virus, which causes 2019 Coronavirus Disease, COVID-19. The motivation for this proposal is the use of an electrical impedance tomography system for online visualization of Positive Expiratory End Pressure (PEEP) in patients with severe symptoms of the disease. Another justification for the development of this tomography system is found in the high number of patients and the high cost of the CT examination. With that, we propose that the EIT can be used to obtain useful results similar to those of an MRI or computed tomography. The equipment needed to perform the EIT is already well known for being much cheaper and easier to transport than an MRI or computed tomography device. In EIT, when the tissue is excited by an alternating current in a frequency range, an electrical potential is generated in the conductive volume under study.

This current injection occurs between two neighboring electrodes and the voltage measurement is performed by two other electrodes, adjacent or not. The EIT does not use ionizing radiation, which offers safety to the patient, as it can be used in the treatment of neoplasms and mechanical ventilation, by means of a disposable silicone electrode strap that must be placed on the patient's chest.

The objective of the present work is to test the two-dimensional D-Bar algorithm, developed by Siltanen (2017) to use it in a low cost multifrequency EIT system for the future monitoring of COVID-19 in ICU beds.

II. MATERIALS AND METHODS

The objective of the two-dimensional D-Bar method is to obtain internal images of cross sections of patients whose body is surrounded by a 16 electrode band. A certain voltage potential was maintained at each electrode and measurements of the resulting electric current through the electrodes were collected. This measurement is repeated for several voltage patterns. Numerical phantoms of radial sections were used with the presence of the lungs and the heart.

Assuming that there are 16 electrodes in total, we can use a maximum of 14 linearly independent voltage patterns, since one of the electrodes is considered the potential of the earth and the other potentials are compared to that of the earth. In the tested algorithm, trigonometric voltage patterns approximated by continuous sinusoidal curves in the contour were used. The conductivities of the heart and lungs were simulated in the first two files that are rotated and then the maps of Dirichlet-Neumann and Neumann-Dirichlet are generated. According to Siltanen (2017) the solution to the conductivity equation is given as a linear combination of basic functions that are linear by parts in a triangular mesh. The mesh is constructed by the `mesh_comp.m` routine containing the `Nrefine` parameter. Here we use `Nrefine = 5`.

In this work, we use the two-dimensional D-Bar method scripts developed by Siltanen et al. (2017) to generate some test images [27].

We will show how to simulate the voltage data for current distribution and how to recover the internal conductivity of the contours, using two-dimensional D-bar method. The algorithms were obtained from the following website: <https://blog.fips.fi/author/samu/>. The codes were compiled in the following sequence:

- (1) `heartNlungs.m`;
- (2) `DbarEIT01_heartNlungs_plot.m`;
- (3) `DbarEIT02_mesh_comp.m`;
- (4) `FEMconductivity.m`;
- (5) `DbarEIT03_ND_comp.m`;
- (6) `DbarEIT04_Kvec_comp.m`;
- (7) `DbarEIT05_psi_BIE_comp.m`;
- (8) `solveBIE.m`;
- (9) `DbarEIT06_tBIE_comp.m`;
- (10) `DbarEIT07_tBIRecon_comp.m`.

The objective of the two-dimensional D-Bar method is to obtain internal images of cross sections of patients whose body is surrounded by a 16 electrode band. A certain voltage potential was maintained at each electrode and measurements of the resulting electric current through the electrodes were collected. This measurement is repeated for several voltage

Later, we intend to apply these images in a low-cost EIT system, for monitoring respiratory diseases and COVID-19, as well as their variants, at the edge of ICU beds. The computer used was a Centrium with an Intel Xeon processor, CPU E3-1231 v3, 3.4 GHz and 16 GB of RAM.

III. RESULTS AND DISCUSSION

The images were reconstructed from original images simulated in Matlab 2013b. Several sets of conductivity have

been defined for the lungs and the heart, in order to simulate the most unusual images of respiratory and cancerous pathologies.

The normal conductivities of the lungs are around 0.5 S/m and corallation 2.0 S/m. Remembering that the conductivity of the background (white) of the image is 1 S/m.

Fig. 1 shows the lungs with electrical conductivity of 0.1 S/m and the heart with 3.5 S/m. The image on the right is the original (simulated) and the image on the left is the reconstructed image. Under these conditions, the reconstructed image has good spatial resolution and well-defined contours.

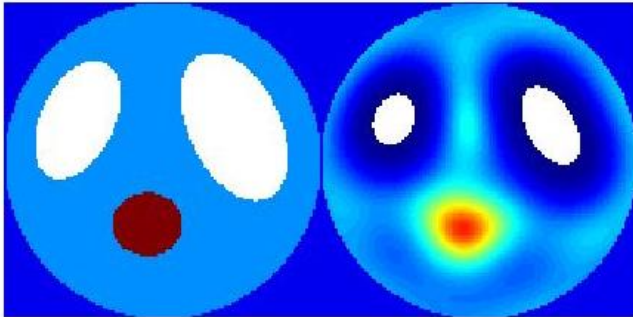


Fig. 1. Lungs with electrical conductivity of 0.1 S/m and the heart with 3.5 S/m.

Fig. 2 shows the lungs with electrical conductivity of 0.4 S/m and the heart with 6.0 S/m. We see that the image shows no discontinuities. It can be noted that the magnitude of the organs, especially the lungs, is smaller in the reconstructed image.

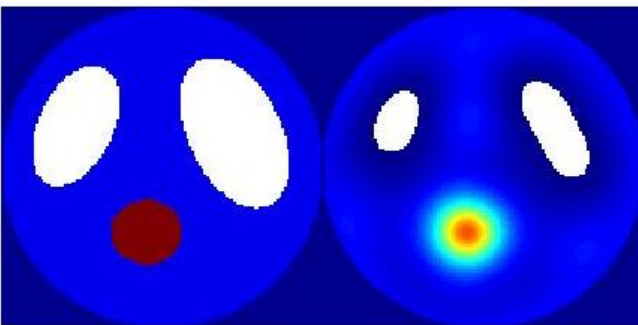


Fig. 2. Lungs with electrical conductivity of 0.4 S/m and the heart with 6.0 S/m.

Fig. 3 shows the lungs with electrical conductivity of 5 S/m and the heart with 20 S/m. Here, we see that the reconstructed image presents discontinuities in three regions.

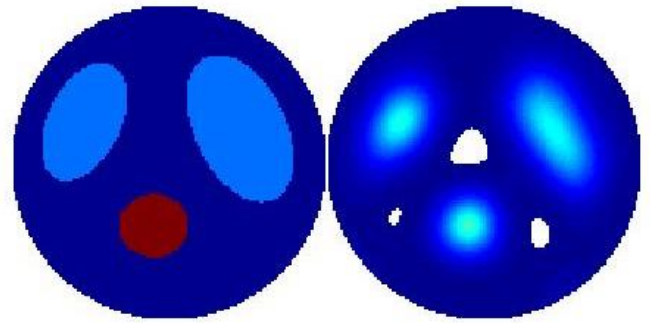


Fig. 3. Lungs with electrical conductivity of 5 S/m and the heart with 20 S/m.

Fig. 4 shows the lungs with electrical conductivity of 1.2 S/m and the heart with 2.0 S/m.

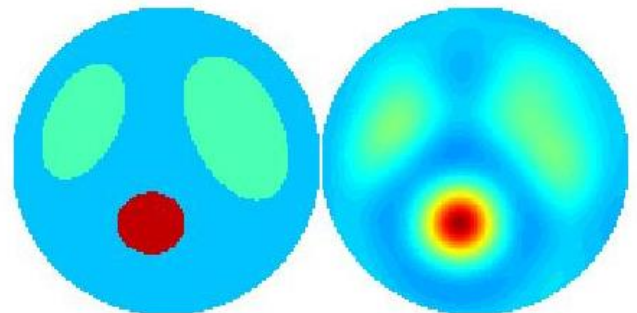


Fig. 4. Lungs with electrical conductivity of 1.2 S/m and the heart with 2.0 S/m.

Fig. 5 shows two extreme cases where the lungs have an electrical conductivity of 0.01 S/m and the heart has conductivity of 28.0 S/m.

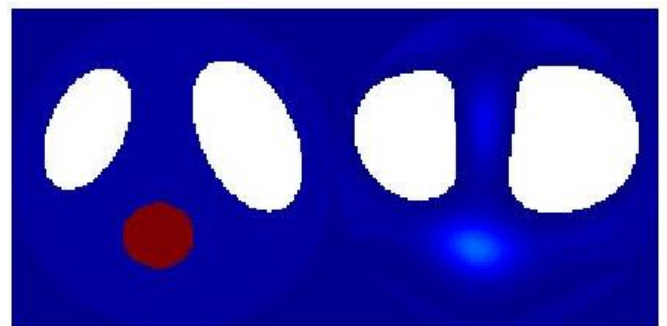


Fig. 5. Lungs with electrical conductivity of 0.01 S/m and the heart has conductivity of 28.0 S/m.

Fig. 6 shows the lungs at 10 S/m and the heart at 4.0 S/m. Note that in this configuration the reconstructed image also has a small region of discontinuity.

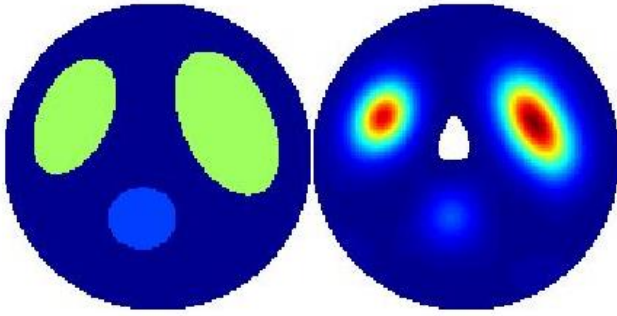


Fig. 6. Lungs with electrical conductivity of 10 S/m and the heart with 4.0 S/m.

Fig. 7 shows the lungs at 15 S/m and the heart at 8.0 S/m. It was concluded that for this configuration, the reconstructed image presents several regions with conductivity 1.0 S/m, which does not correspond to the original image. However, we can still visualize the heart and lungs very well.

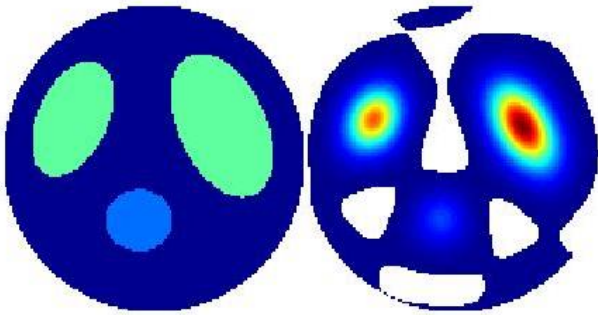


Fig. 7. Lungs with electrical conductivity of 15 S/m and the heart with 8.0 S/m.

IV. CONCLUSION

The two-dimensional D-Bar method has shown promising results in 2D reconstruction of electrical impedance tomography images. The colors of the simulated and reconstructed original images represent the numerical values of conductivity in the organs and, therefore, are directly comparable. Note that reconstruction underestimates the magnitude of electrical conductivity in the heart. This is a characteristic of the truncated Fourier nonlinear transform, calculated in the D-Bar method, already predicted by Siltanen (2017) [27]. He approached the 3D situation from the D-Bar method to a 2D computational model. In practice, this model generates relevant and quick results. The experimental results show that the method can be used to monitor PEEP and other pulmonary activities in patients positive for COVID-19 as a support device. Seven completely different scenarios were simulated in Matlab to prove the effectiveness and robustness of the algorithm. Each image took about 11 minutes to be reconstructed. As a future work, it is intended to accelerate the two-dimensional algorithm used in the D-Bar method made by Siltanen (2017) using a deep neural network,

training the network using a set of synthetic images modeled as numerical phantoms of the lungs and heart in radial section [27].

ACKNOWLEDGMENT

The authors thank UDESC, UFPE and FAPESC for their assistance. Special thanks to professor and researcher Samuli Siltanen (Finland) for sharing his knowledge with the scientific community.

REFERENCES

- [1] Martins, T. de C. et al. (2019) A review of electrical impedance tomography in lung applications: Theory and algorithms for absolute images. *Annual Reviews in Control*, 48: 442-471.
- [2] Maisch, S.; et al. (2011) Heart–lung interactions measured by electrical impedance tomography. *Brief Communications. Crit. Care Med.*, v. 39, n. 9, p. 2173-2176.
- [3] ROMSAUEROVA, A. et al. (2006) Multi-frequency electrical impedance tomography (EIT) of the adult human head: initial findings in brain tumours, arteriovenous malformations and chronic stroke, development of an analysis method and calibration. *Physiological Measurement*, v. 27, S147-S161. DOI:10.1088/0967-3334/27/5/S13.
- [4] S. Leonhardt, R. Pikkemaat, O. Stenqvist and S. Lundin. (2012) Electrical Impedance Tomography for hemodynamic monitoring. In: 2012 Annual International Conference of the IEEE Engineering in Medicine and Biology Society, p. 122-125. DOI: 10.1109/EMBC.2012.6345886.
- [5] Mangnall, Y. F.; Kerrigan, D. D.; Johnson, A. G.; Read, N. W. (1991). Applied Potential Tomography Noninvasive Method for Measuring Gastric Emptying of a Solid Test Meal. *Digestive Diseases and Sciences*, vol. 36, n. 12, pp. 1680-1684.
- [6] Zhao, Z.; Kung, W-H.; Chang, H-T.; Hsu, Y-L.; Frerichs, I. (2020) COVID-19 pneumonia: phenotype assessment requires bedside tools. *Critical Care*, v. 24, n. 272. DOI: <https://doi.org/10.1186/s13054-020-02973-9>.
- [7] Heizmann S., Baumgärtner M., Krüger-Ziolek S., Zhao Z., Möller K. (2014) 3-D Lung Visualization Using Electrical Impedance Tomography Combined with Body Plethysmography. In: Goh J. (eds) *The 15th International Conference on Biomedical Engineering. IFMBE Proceedings*, vol 43. Springer, Cham. https://doi.org/10.1007/978-3-319-02913-9_44.
- [8] Trokhanova, O. V.; Chijova, Y.A.; Okhapkin, M. B.; Korjensky, A. V.; Tuykin, T. S. (2010) Using of electrical impedance tomography for diagnostics of the cervix uteri diseases. *Journal of Physics: Conference Series*, v. 224, 012068. DOI:10.1088/1742-6596/224/1/012068.
- [9] M. Glidewell and K. T. Ng (1995) Anatomically constrained electrical impedance tomography for anisotropic bodies via a two-step approach, in *IEEE Transactions on Medical Imaging*, vol. 14, no. 3, pp. 498-503, Sept. 1995. DOI: 10.1109/42.414615.
- [10] J. Nasehi Tehrani , T.I. Oh , C. Jin , A. Thiagalingam, A. McEwan. (2012) Evaluation of different stimulation and measurement patterns based on internal electrode: Application in cardiac impedance tomography. *Computers in Biology and Medicine*. vol. 42, no. 11, November 2012, p. 1122-1132.
- [11] Woo E J, Hua P, Webster J G, Tompkins W J (1993) A robust image reconstruction algorithm and its parallel implementation in electrical impedance tomography. *IEEE Trans. Med. Imaging*, 12:137-46
- [12] Cohen-Bacrie C., Goussard Y, Guardo R (1997) Regularized reconstruction in electrical impedance tomography using a variance uniformization constraint. *IEEE Trans. Med. Imaging*, 16(5): 562-71
- [13] Vauhkonen M, Vadasz D, Karjalainen P A, Somersalo E, Kaipio J P (1998) Tikhonov regularization and prior information in electrical impedance tomography. *IEEE Trans. Med. Imaging*, 17: 285-93
- [14] Jin B, Khan T, Maass P (2012) A reconstruction algorithm for electrical impedance tomography based on sparsity regularization. *Int. J. Numer. Methods Eng.*, 89:337-53

- [15] Gehre M, Kluth T, Lipponen A, Jin B, Seppanen A, Kaipio J P, Maass P (2012) Sparsity reconstruction in electrical impedance tomography: An experimental evaluation. *J. Computat. Appl. Math.*, 236: 2126–36
- [16] Yang Y, Wu H, Jia J. (2017) Image reconstruction for electrical impedance tomography using enhanced adaptive group sparsity with total variation. *IEEE Sens. J.*, 17: 5589–98
- [17] Zhang K, Li M, Yang F, XU S, Abubakar A. (2019) Three-dimensional electrical impedance tomography with multiplicative regularization. *IEEE Trans. Biomed. Eng.*, 66: 2470–8
- [18] Brandstätter B; Hollaus K, Hutten H, Mayer M, Merwa R, Scharfetter H (2003) Direct estimation of Cole parameters in multifrequency EIT using a regularized Gauss–Newton method. *Physiological Measurement*, 24(2): 437
- [19] Hadinia M, Jafari R, Soleimani M (2016). EIT image reconstruction based on a hybrid FE-EFG forward method and the complete-electrode model. *Physiological Measurement*, 37(6). <https://doi.org/10.1088/0967-3334/37/6/863>
- [20] Adler A; Boyle A (2017) Electrical Impedance Tomography: Tissue Properties to Image Measures. *IEEE Trans Biomed Eng Nov*; 64(11): 2494-2504. DOI: 10.1109/TBME.2017.2728323
- [21] Patino N M, Valentinuzzi M (1995) Reconstruction algorithm for electrical impedance tomography based on the linear approximation method. In: *Engineering in Medicine and Biology Society*, 1995. In: *Proceedings of the 20th Annual International Conference of the IEEE*, v. 1, pp. 561–562
- [22] Siltanen S (1999) *Electrical impedance tomography and Faddeev Green's functions*. Ann. Acad. Sci. Fenn. Math. Diss. 121. PhD. Dissertation Helsinki University of Technology
- [23] Shin K, Mueller J L (2020) A second order Calderon's method with a correction term and a priori information. *Inverse Problems*. Accepted Manuscript
- [24] Santos T B R, Nakanishi R M, Kaipio J P, Mueller, J L, Lima R G (2020) Introduction of sample based prior into the D-bar method through a Schur complement property. *IEEE Transactions on Medical Imaging* (Early Access)
- [25] Hamilton S J, Isaacson D, Kolehmainen V, Muller P A, Toivanen J, Bray P F (2020) 3D EIT reconstructions from electrode data using direct inversion D-bar and calderon methods. <https://arxiv.org/pdf/2007.03018.pdf>
- [26] Siltanen S, Mueller J, Isaacson D (2000) An implementation of the reconstruction algorithm of A Nachman for the 2-D inverse conductivity problem. *Inverse Problems*, 16: pp. 681–99
- [27] Siltanen S (2017) The D-bar Method for Electrical Impedance Tomography – Simulated Data. Available in: <https://blog.fips.fi/tomography/eit/the-d-bar-method-for-electrical-impedance-tomography-simulated-data/>. Access in: 28 dez. de 2020.
- [28] Dodd M and Mueller J L (2014) A Real-time D-bar Algorithm for 2-D Electrical Impedance Tomography Data. *Inverse Probl Imaging*, 8(4):1013–1031. DOI:10.3934/ipi.2014.8.1013.